Pattern Formation in the Methylene-Blue−Glucose System

A. J. Pons,[†] F. Sagués,[‡] M. A. Bees,[§] and P. Graae Sørensen*,[||]

Department of Chemistry, H. C. Ørsted Institute, University of Copenhagen, Universitetsparken 5, DK-2100 Copenhagen, Denmark, Departament de Química Física, Universitat de Barcelona, Martí i Franqués 1, 08028 Barcelona, Spain, and Department of Mathematics and Statistics, University of Surrey, Guildford, GU2 5XH, U.K.

Received: October 6, 1999; In Final Form: December 22, 1999

We report a systematic study of pattern formation in a thin fluid layer driven by a simple chemical reaction. The hydrodynamic instability arises due to the increase of fluid density in the subsurface layer caused by the O_2 oxidation of glucose to gluconic acid with the methylene blue as a catalyst. We also report independent measurements of the kinetics of the reaction and of the increase in density which gives rise to the instability.

1. Introduction

Several mechanisms of pattern formation have previously been investigated in chemical systems. The most paradigmatic examples involve complex kinetics with an autocatalytic process coupled to the diffusion of the reactants and have been widely studied experimentally and theoretically, giving rise to propagating waves or to stationary patterns (Turing structures). If special precautions are not taken the patterns are sometimes influenced by bulk motion of the fluid, with a substantial increase in the complexity of the modeling. Among several hydrodynamic interactions, Marangoni-type motions induced by surface tension gradients,[1] Rayleigh−Benard type convection driven by density gradients induced by temperature,[2] and density gradients directly generated by chemical reactions,[3] have been mostly analyzed. Spatial patterns have also been described at liquid interfaces (for a brief summary see ref 4). In a pioneering work, Möckel[5] observed the appearance of inhomogeneous concentration stripes while irradiating the KI/CCl_4 starch system in water. More recently after experimental work by Micheau et al.[6] and Avnir et al.,[7] this phenomenon has been demonstrated to be much more general, not only to create photochemical structures at liquid/air interfaces, but also for reactions at gas/liquid interfaces and even when reagents in the same solvent are separated by a dialysis membrane. In the case of photolysis of halogen compounds in open Petri dishes, preexisting convection produced by Marangoni-like instabilities seems to be predominant. In other cases, the most well-known being the photoreduction of ferric ion by oxalic acid followed by complexation to a blue dye known as Turnbull's blue,[7] spectacular patterns are seen in a covered dish and have been interpreted in terms of a double diffusion mechanism.[4] Spatial patterns have also been described at liquid interfaces due to other mechanisms (i.e., vertical concentration gradients[8] or mixed mechanisms[9]).

In this paper, we describe a system where the kinetics are very simple and where the main mechanism for pattern formation is a gravitational instability generated by an increase in the density of the fluid layer just below the surface of the reaction mixture. The chemical reaction is well-known and is sometimes referred to as "the blue bottle experiment".[10,11] It is an alkaline oxidation of glucose by oxygen with methylene blue as catalyst and indicator. We assume that the main oxidation product is gluconic acid. During the reaction a gradual accumulation of gluconic acid increases the local density of the solution.

Oxygen is supplied continuously to the system from the atmosphere, diffusing through the surface layer, and is consumed by the reaction. Since the homogeneous initial conditions correspond to a large deficiency in oxygen in the reaction mixture, the extent of the reaction, and thus the corresponding density gradient, increases with time and decreases with the fluid depth, eventually causing a hydrodynamic instability. The instability produces a pattern of blue dots and/or lines of oxygen-rich sinking fluid and colorless oxygen-poor rising fluid between these lines or dots. This pattern appears after minutes or a few hours depending on the rate constants of the chemical reaction. Our aim in this paper is to initiate a study of this pattern formation phenomenon using pH, concentration of glucose, total concentration of catalyst, temperature, and depth as control parameters.

Although the reaction is slightly exothermic, the instability cannot be of a Rayleigh−Bernard type because the major production of gluconic acid (and hence the production of heat) is near the top of the layer of fluid instead of the bottom. Nevertheless, it is important to thermostat the system very carefully and remove the heat produced by the reactions.

Chemical systems using other saccharides (e.g., D-xylose or D-galactose) and indicators (e.g., toluidine blue) can produce similar results.[12,13]

The system is formally similar to bioconvection in a suspension of swimming microorganisms, whose individual motions are biased upward and are denser than the fluid in which they swim. The microorganisms tend to accumulate close to the surface and this gives rise to an overturning instability.[14,15]

The paper is organized as follows. In section 2 we describe the experimental methods. In section 3 we present the results of the kinetics experiments, the measurement of density differences of glucose/gluconic acid solutions and the experiments measuring the evolution in time of the concentration of O_2, and finally we describe the patterns and how they change with the different experimental parameters. In section 4 we propose a simplified kinetic model for the homogeneous system. In section

* Corresponding author.
[†] Copenhagen University and Universitat de Barcelona. E-mail: apr@kiku.dk.
[‡] Universitat de Barcelona. E-mail: f.sagues@qf.ub.es.
[§] University of Surrey. E-mail: m.bees@surrey.ac.uk.
[||] Copenhagen University. E-mail: pgs@kiku.dk.

10.1021/jp9935788 CCC: $19.00
Published on Web 02/18/2000

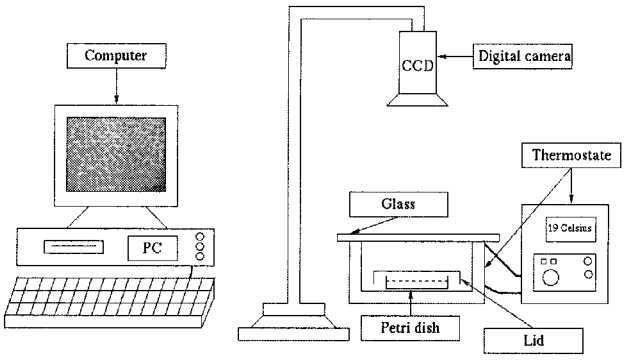

Figure 1. Experimental setup to study the patterns.

5 we model the reaction−diffusion equations with zero fluid flow, and in section 6 we discuss the origin of the patterns. Finally, in section 7 we give some conclusions and future perspectives.

2. Experimental Section

2.1. Materials. Double ion-exchanged water was used throughout. NaOH (Merck A109956), analytical grade D(+)-glucose (Merck A108337)) and methylene blue (Fluka A55631) were used without further purification.

2.2. Equipment. The investigation of the reaction mechanism was done in a HP8453A diode array spectrophotometer equipped with a cuvette holder thermostated at 19.0 °C to within ±0.1 °C by a Heto CB 8−30 thermostat. After thorough mixing of the pre-thermostated reactants a 1 cm cuvette was filled completely with the solution, covered with a lid, and inserted in the cuvette holder. The absorbance at 662 nm, corresponding to the absorption maximum of MB^+, was measured as a function of time using the HP8453 kinetics program.

The study of the evolution of O_2 diluted in the solution was performed in a thermostated 1 cm square cuvette. The oxygen concentration was measured with an MI-730 oxygen microelectrode from Microelectrodes Inc. connected to a Keithley 485 picoamperemeter. We worked with an inert atmosphere of N_2 above the cuvette to prevent the O_2 entering into the cuvette through the hole for the electrode.

The density of solutions of glucose and of gluconic acid was measured using a 25 mL Gay-Lussac pycnometer. The measurements were made at 25.0 ± 0.1 °C and were reproducible to within ±0.0005 g/cm^3. A Branson 1210 ultrasonic bath was used to remove air bubbles from the pycnometer fluid.

The patterns were studied in a covered Petri dish with inner diameter 18.5 cm and height 2.7 cm. The depth of the liquid layer was 0.8 cm except where indicated otherwise. During the experiments the Petri dish was inserted in a glass plate covered cylindrical container which was thermostated at 19.0 °C to within ±0.1 °C except where indicated otherwise. It is quite important to cover the Petri dish with a lid to prevent air movement that could perturb the system. Pictures of the pattern were taken by a computer-controlled CCD-9230 camera, and the pictures were stored on the computer disk. (See Figure 1). The width of all pictures corresponds to 13.5 cm except where indicated otherwise.

2.3. Procedure for Preparing the Reaction Mixture. Water, 1 M NaOH, 0.03126 M MB^+, and glucose were mixed to obtain the desired concentrations. Then the solution was thermostated for half an hour, after which it was shaken so as to be saturated with oxygen and finally poured into the cuvette or the Petri dish.

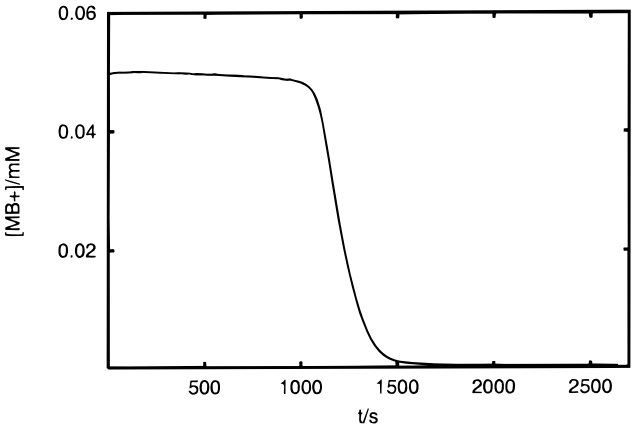

Figure 2. Timetrace of absorbance of a homogeneous system at 20.0 °C. Initial mixture: $[OH^-] = 0.020$ M, $[MB^+] = 4.6 \times 10^{-5}$ M, [GL] = 0.054 M.

3. Experimental Results

3.1. Kinetics of the Homogeneous Reaction. For the range of pH used in this study (pH 9−13), gluconic acid (GLA) is the main product when glucose (GL) is oxidized, with methylene blue as a catalyst. The main reaction steps are

$$O_2 + 2MBH \rightarrow 2MB^+ + 2OH^- \quad (1)$$

$$GL + MB^+ + OH^- \rightarrow MBH + GLA \quad (2)$$

where MB^+ and MBH are the blue oxidized and the colorless reduced forms of methylene blue, respectively. When a clear sample of reaction mixture is shaken with air it becomes blue immediately while the return to the white state is slow. This can be explained by assuming that the rate of reaction 1 is much larger than the rate of reaction 2 when the mixture is saturated with air.

In a typical experiment the initial concentrations are as follows. [GL] = 0.054 M, $[OH^-] = 0.02$ M, $[MB^+] + [MBH] = 4.6 \times 10^{-5}$ M, and $[O_2] = 2.6 \times 10^{-4}$ M. The initial concentration of O_2 may be estimated from the solubility of O_2 in air-saturated water. As the initial concentration of O_2 is larger than the total concentration of the catalyst, all methylene blue is immediately converted to the blue form MB^+. The concentrations of GL and OH^- can be considered constant during the reaction as they are present in much larger concentrations than O_2.

We have measured the time dependence of $[MB^+]$ in a homogeneous and closed system (without a supply of oxygen diffusing in from the atmosphere) using a spectrophotometer. The timetrace of homogeneous absorbance measurements for this system is shown in Figure 2. After mixing, the absorbance remains almost constant until the initial amount of oxygen is used up. During this phase, reactions 1 and 2 are occurring simultaneously. In the second phase, the decrease in $[MB^+]$ is determined by reaction 2 alone. During this phase $[MB^+]$ is decreasing exponentially, showing that the rate of reaction 2 is first order in $[MB^+]$. The rate of reaction 2 is very dependent on $[OH^-]$, as explained later.

We have also measured the time dependence of $[O_2]$ using a microelectrode. The result for the standard mixture is shown in Figure 3.

3.2. Density Measurements. The measurements were performed using a 25 mL Gay-Lussac pycnometer. For calibration the pycnometer was filled with pure water, thermostated at 25.0

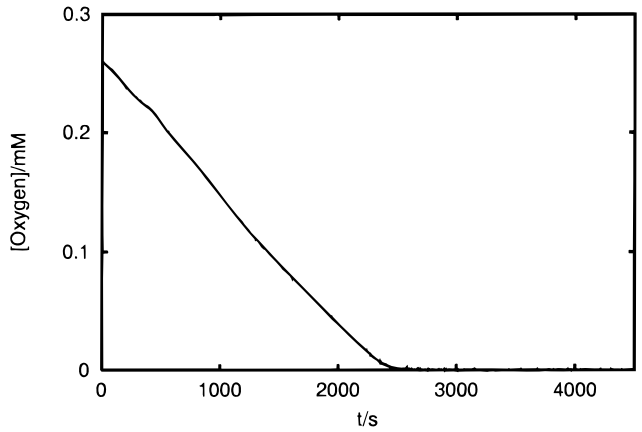

Figure 3. Timetrace of oxygen electrode in a homogeneous system at 19.0 °C. Initial mixture: $[OH^-] = 0.020$ M, $[MB^+] = 4.6 \times 10^{-5}$ M, $[GL] = 0.054$ M.

°C, and the air bubbles were removed using an ultrasonic bath. Then it was thermostated for 10 min. After insertion of the stopper the filled pycnometer was carefully dried and weighed. The calibration was repeated until consistent results were obtained. This procedure was then repeated with two different 0.055 M solutions of glucose and gluconic acid. The densities of the two solutions were calculated using the known density of water at 25.0 °C (i.e., 0.9970480 g/mL) and the results are the following: ρ_{GL} (25 °C) = 1.0008 ± 0.0005 g/mL and ρ_{GLA} (25 °C) = 1.0032 ± 0.0005 g/mL.

3.3. Evolution of Patterns. The typical development of a pattern is as follows. After saturation with oxygen the homogeneous blue mixture is poured into the Petri dish. At the beginning the liquid appears as a homogeneous blue fluid layer. But, after some time, the color disappears except in a top layer of the order of one mm.

The pattern emerges after a transient stage which lasts between 20 min to several hours depending on the experimental conditions. When viewed from above, it initially looks like blue patches on a softer blue background. After some time the patches become deeper blue and the background looks colorless. Looking directly from the side the dark blue patches can be seen as tongues of blue liquid slowly sinking to the bottom while colorless fluid is moving upward between them. Sometimes the sinking tongues appear, when viewed from the side, as sheets of blue fluid. These sheets look like blue lines when seen from above. After their onset, the patterns generally remain stationary, but lines have a tendency to break up into a series of patches or dots.

Normally, the pattern consists of an ensemble of circulation cells appearing as a disordered array of blue dots of slightly different sizes or a set of lines (sometimes mixed with dots) that are neither straight nor ordered. The evolution of the pattern in time is quite dependent on the rate constants. The main interaction between dots is a slow unification or separation.

A slow drift can be seen in some cases spreading or squeezing the pattern toward the center of the Petri dish. In other cases the dot/line-shaped pattern does not fill the whole Petri dish but is confined to the middle region. Insufficient lateral thermostatic conditions may also lead to pronounced global inhomogeneities.

After some time the pattern becomes less visible. The first sign of this is that some of the blue dots become colorless. This behavior starts at the center of the Petri dish and spreads slowly to the walls. Finally, the layer becomes homogeneous again and it appears light blue.

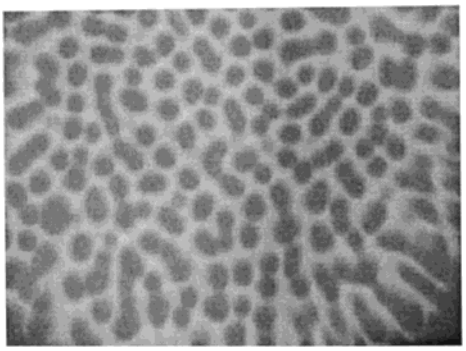

Figure 4. Typical dot-shaped pattern. Initial mixture: $[OH^-] = 0.020$ M, $[MB^+] = 4.6 \times 10^{-5}$ M, $[GL] = 0.054$ M. Depth ≈ 7 mm. The width of the picture is 13.5 cm and it was taken 6000 s after starting the experiment.

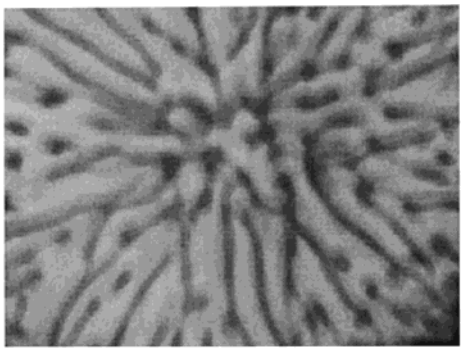

Figure 5. Typical line-shaped pattern. Initial mixture: $[OH^-] = 0.020$ M, $[MB^+] = 4.6 \times 10^{-5}$ M, $[GL] = 0.054$ M. Depth ≈ 15.5 mm. The picture was taken 4000 s after starting the experiment.

Two typical fully developed patterns are shown in Figures 4 and 5 corresponding, respectively, to situations where dotted or striped configurations dominate. Usually we can distinguish two different length scales in the patterns, the dot (or line) thickness and the distance between dots or lines. These two length scales are clearly linked such that if one of the scales increases the other usually decreases and vice versa.

3.4. Influence of Control Parameters on Patterns. *Dependence on pH.* The pH is with no doubt the most important parameter that controls the appearance of the pattern. The main reason for this is that the rates of reactions 1 and 2 depend strongly on $[OH^-]$, as demonstrated later. The higher the values of the reaction rates, the faster the dynamical process that builds up the pattern and makes it disappear again. Figure 6 shows typical patterns for different initial values of $[OH^-]$.

From the experiments it is readily seen that the dot size decreases and that the distance between dots (or lines) increases with $[OH^-]$. A common feature for high values of $[OH^-]$ is that lines dominate over dots when the pattern emerges and that lines break into dots after some time. The concentration of OH^- at which a transition can be observed from dot-shaped initial patterns to line-shaped initial patterns is between 0.050 and 0.060 M.

Figure 7 shows the dependence on the $[OH^-]$ of the time needed for the pattern to emerge. To estimate this time we have increased the contrast of the pictures and recorded the time corresponding to the first picture which unambiguously deviated from the previous one. In the range of $[OH^-]$ where the lines dominate over dots the estimated emergence time is almost independent of $[OH^-]$.

Dependence on Glucose Concentration. Figure 8 shows that the dot size and separation distance do not depend very much

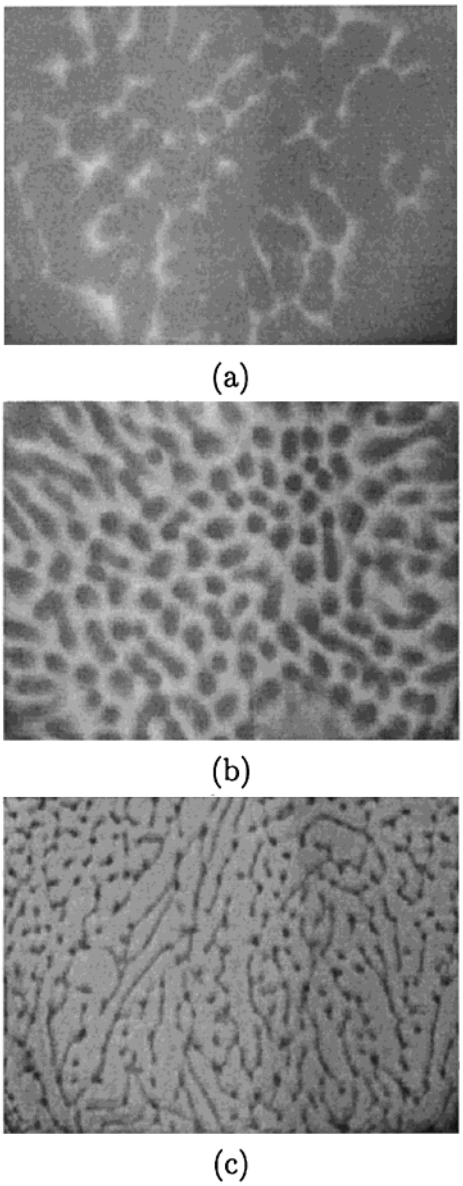

Figure 6. Typical patterns for various initial [OH^-]. Initial mixture for panel (a): [OH^-] = 0.012 M, [MB^+] = 4.6×10^{-5} M, [GL] = 0.054 M, and the picture was taken 8700 s after starting the experiment. For (b), [OH^-] = 0.020 M and the picture was taken 6000 s after starting the experiment. For (c), [OH^-] = 0.073 M and the picture was taken 1120 s after starting the experiment.

on the glucose concentration within the examined range. In some of the experiments local homogeneous areas without patterns were observed to persist after the pattern had developed in the rest of the system. This phenomenon has also been observed in other experimental series, but we have not been able to predict when it will appear. When present, homogeneous areas never develop from a preexisting pattern. A typical example is shown in Figure 8b.

Dependence on the Concentration of Catalyst. Figure 9 shows patterns at different total concentrations of the catalyst. For [MB^+] $\geq 1.1 \times 10^{-4}$ M some crystals of MBH precipitate. This precipitation does not seem to affect the pattern. Another obvious characteristic of these patterns is that at high [MB^+] the blue color observed is darker than it is for lower concentrations of methylene blue.

Dependence on Depth of Fluid Layer. Figure 10 indicates that the dot size may decrease with increasing depth of the fluid layer. The distance between the dots appears, however, to increase. We have found a lower depth threshold for the pattern formation $\approx$ 4 mm.[12] [Panel (a) of Figure 10 is just above that threshold.] Above the threshold the patterns consist almost exclusively of dots. When we approach a depth of 1 cm, elongated dots appear that are similar to short lines. Only for deep systems (depth $\geq$ 13.5 mm) do narrow lines dominate the pattern. The transition between these two kinds of pattern is gradual. Generally, the distance between lines is bigger than the distance between dots. Eventually the lines break into dots.

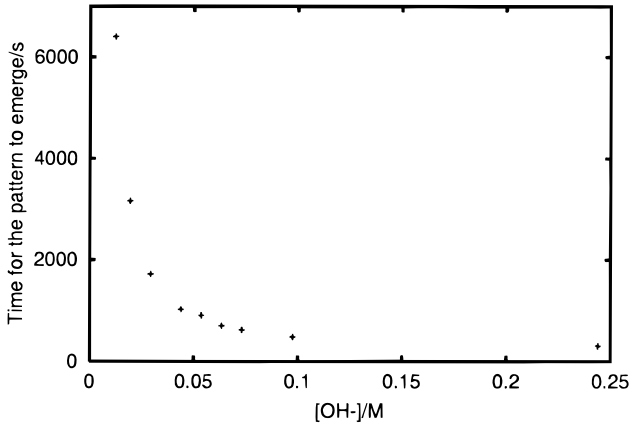

Figure 7. Time needed for the pattern to emerge for different [OH^-].

Dependence on Temperature. Figure 11 shows that the dot size decreases on average with temperature and that the distance between dots increases. At elevated temperatures some water evaporates from the solution, but for systems thermostated below 20 °C this evaporation is not problematic or significant.

Above 20 °C some water vapor is deposited on the lid that covers the Petri dish. This is caused by imperfect thermostatic conditions and makes it difficult to take pictures of patterns at high temperatures. In this case we have also observed a gradual transition from dots to lines, occurring between 23 °C and 24 °C.

4. Determination of Rate Constants for the Kinetic Model

With initial concentrations given in the Experimental Section, the rate-of-change of concentration due to reactions 1 and 2 can be modeled by assuming simple rate laws of the form

$$v_1 = k_1[O_2][MBH] \quad \text{and} \quad v_2 = k_{obs}[MB^+] \qquad (3)$$

respectively. The results of a model calculation using the typical concentrations employed in the kinetic experiments are shown in Figures 12a,b,c. Our theoretical predictions are remarkably consistent with the experimental results (see Figure 12a and Figure 3, respectively). In some cases it was necessary to fit the initial concentration of oxygen to obtain a better fit. This is because we cannot completely control the initial amount of oxygen dissolved in the sample by shaking before starting the measurements.

Assuming that $k_{obs} = k_2$ [OH^-] [GL], we can fit the rate constants k_1 and k_2 to the absorbance measurements. The best match found for the concentrations stated above at 20.0 °C is displayed in Figure 13. The values of k_1 and k_2 found with this method, for different [OH^-] at 19.0 °C, are presented in Figure 14a,b, respectively. The almost linear dependence of k_1 with [OH^-] up to 0.1 M indicates that reaction 1 in this region is first order in [OH^-].

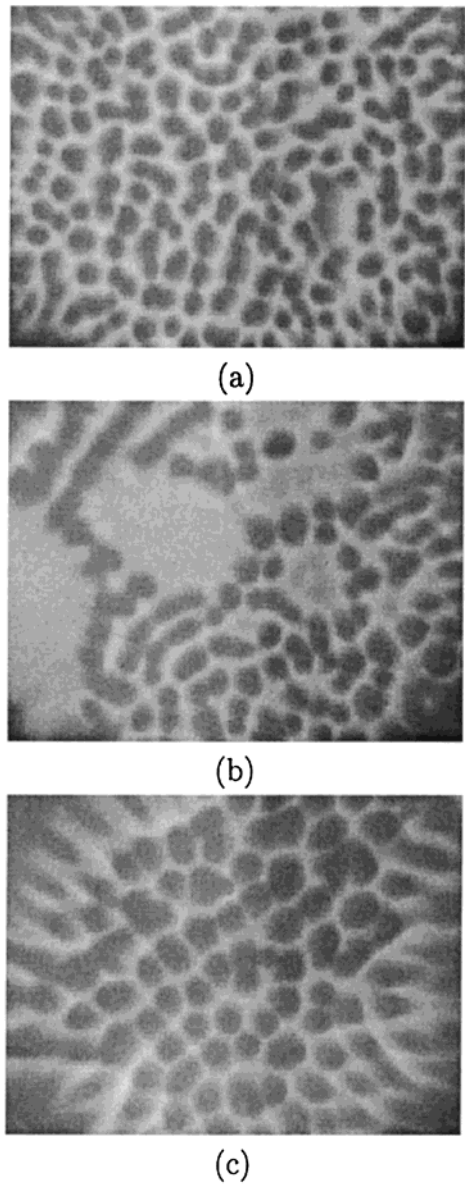

Figure 8. Typical patterns for various initial [GL]. Initial mixture for panel (a): $[OH^-] = 0.020$ M, $[MB^+] = 4.6 \times 10^{-5}$ M, [GL] = 0.027 M, and the picture was taken 7000 s after starting the experiment. For (b), [GL] = 0.108 M and the picture was taken 5000 s after starting the experiment. For (c), [GL] = 0.190 M and the picture was taken 7000 s after starting the experiment.

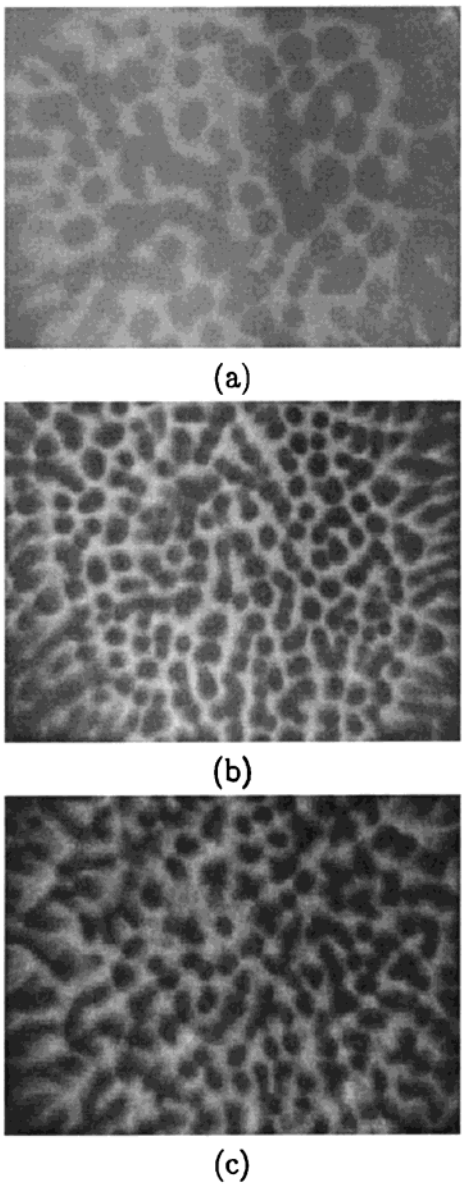

Figure 9. Typical patterns for various initial $[MB^+]$. Initial mixture for panel (a): $[OH^-] = 0.020$ M, $[MB^+] = 1.5 \times 10^{-5}$ M, [GL] = 0.054 M, and the picture was taken 8800 s after starting the experiment. For (b), $[MB^+] = 7.6 \times 10^{-5}$ M and the picture was taken 3600 s after starting the experiment. For (c), $[MB^+] = 2.3 \times 10^{-4}$ M and the picture was taken 9960 s after starting the experiment.

5. Modeling the Reaction−Diffusion System

To check the consistency of our interpretations, we have made a simulation of the one-dimensional reaction−diffusion equation for the system and calculated the concentration/depth profile, assuming that no hydrodynamic convection takes place. In our pattern formation experiments this may be the situation before the pattern appears, particularly for patterns just above the instability threshold. We have used $[O_2]$, $[MB^+]$, and [GLA] as dynamic variables with 2.6×10^{-4} M, 4.6×10^{-5} M, and 0.0 M, respectively, as their initial concentrations. The concentration of MBH is calculated according to $[MBH] = C - [MB^+]$ where C is the total concentration of the catalyst. The concentrations of all other species are considered constant. The $[O_2]$ is fixed at the air−liquid boundary to 2.6×10^{-4} M, which corresponds to the concentration of O_2 in air-saturated water. For all other concentrations we have used no-flux boundary conditions. The expressions (3) are used for the reaction rates with the experimentally determined rate constants $k_1 = 2000$ M^{-1} s^{-1} and $k_{obs} = 0.0042$ s^{-1}. For O_2 we have used the diffusion constant 2.11×10^{-5} cm^2 s^{-1}. As the molecular weights of MB^+ and GLA are much higher than the molecular weight of O_2, the diffusion constants for these species have been set to zero.

The profiles of the dynamic variables after 10066 s are shown in Figure 15. From Figure 15b we can estimate the thickness of the blue layer to be 3 mm, which corresponds quite well to the value observed before the formation of patterns. Figure 15a shows that O_2 is absent below the blue layer. From Figure 15c it is seen that GLA primarily accumulates in the subsurface layer and that the concentration here is approximately equal to 1.9 mM after 10066 s. From the estimated layer thickness the total amount of GLA produced in 1 cm^2 of the layer can be estimated to be 6.6×10^{-7} mol, corresponding to a consumption of O_2 equal to 3.3×10^{-7} mol. This is more than the amount of O_2 initially dissolved in 1 cm^2 of the layer (7.8×10^{-8} mol) but

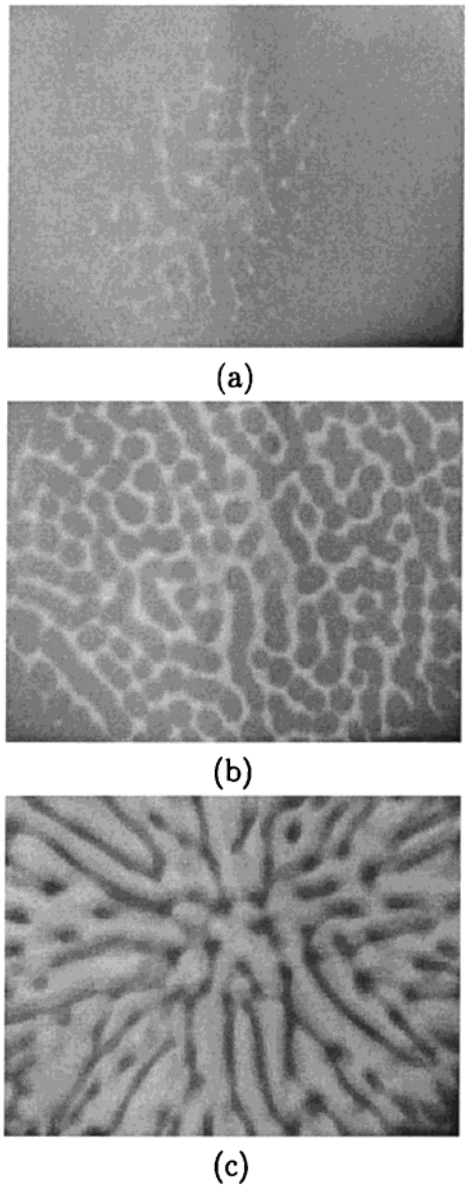

Figure 10. Typical patterns obtained by increasing the depth of the fluid layer. Initial mixture: $[OH^-] = 0.020$ M, $[MB^+] = 4.6 \times 10^{-5}$ M, [GL] = 0.054 M. (a) Depth $\approx$ 4 mm and the picture was taken 5000 s after starting the experiment. (b) Depth $\approx$ 5 mm and the picture was taken 7000 s after starting the experiment. (c) Depth $\approx$ 15.5 mm and the picture was taken 4500 s after starting the experiment.

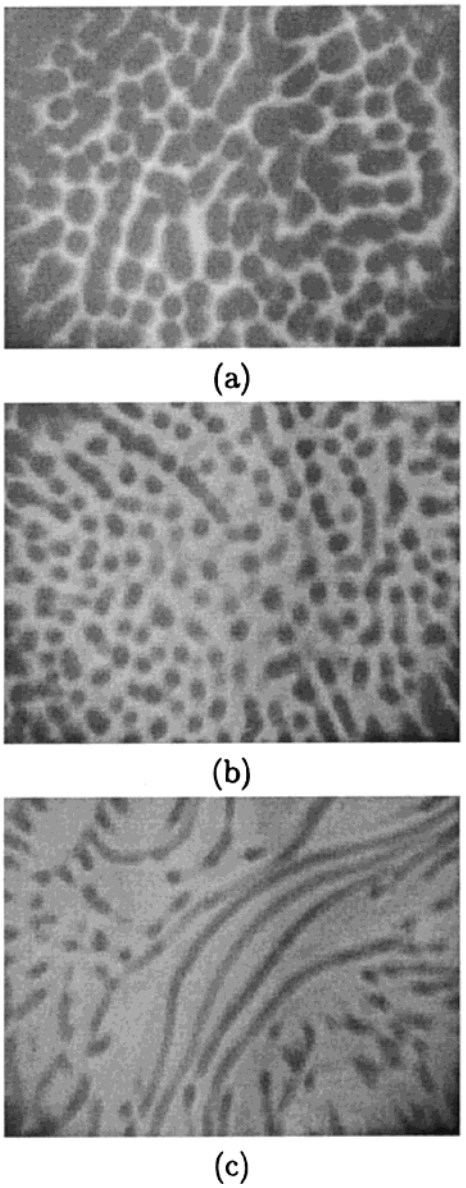

Figure 11. Typical dependence of patterns with variations in the temperature of the system. Initial mixture: $[OH^-] = 0.020$ M, $[MB^+] = 4.6 \times 10^{-5}$ M, [GL] = 0.054 M. (a) Temperature = 17.0 °C. The picture was taken 5500 s after starting the experiment. (b) Temperature = 20.5 °C. The picture was taken 3500 s after starting the experiment. (c) Temperature = 24.0 °C. The picture was taken 2000 s after starting the experiment.

less than the total amount available in a 2 cm air column above the layer (1.7×10^{-5} mol). This confirms that the amount of oxygen in the covered Petri dish is more than sufficient for maintaining the reaction during the experiment. It should also be noticed that the change in [GL] and $[OH^-]$ is small compared to the initial concentrations, thus justifying the assumption of constant concentrations of OH^- and GL in the kinetic model.

6. Interpretation of the Pattern Forming Instability

Currently we lack a quantitative analysis of the phenomenon at hand in terms of wavelength characterization. We can, however, describe qualitatively the origin of the instability behind the formation of the patterns. We propose that the main explanation is an overturning instability. The determination of the density difference between equimolar solutions of glucose and gluconic acid confirms that the local solution density increases when gluconic acid is produced from glucose. We can also state that the main production of gluconic acid occurs in the top layer of the solution where we have a continuous supply of O_2. Evaporation is eliminated by using a covered Petri dish but surface-tension gradients may be present, at least in fully developed systems where horizontal concentration gradients exist in the top layer. As a result, the role of a Marangoni-like instability cannot be completely ruled out. Actually, a Marangoni-induced instability, resulting in pattern formation, in the similar methylene blue−sulfide−oxygen system has been recently reported by Watzl et al.,[16] although in a different experimental arrangement. In the present experiments, however, we believe that the overturning instability constitutes the most important contribution to the hydrodynamic instability. Marangoni effects may play a role in the dot formation or in the setting of specific length scales but does not explain the initial pattern formation.

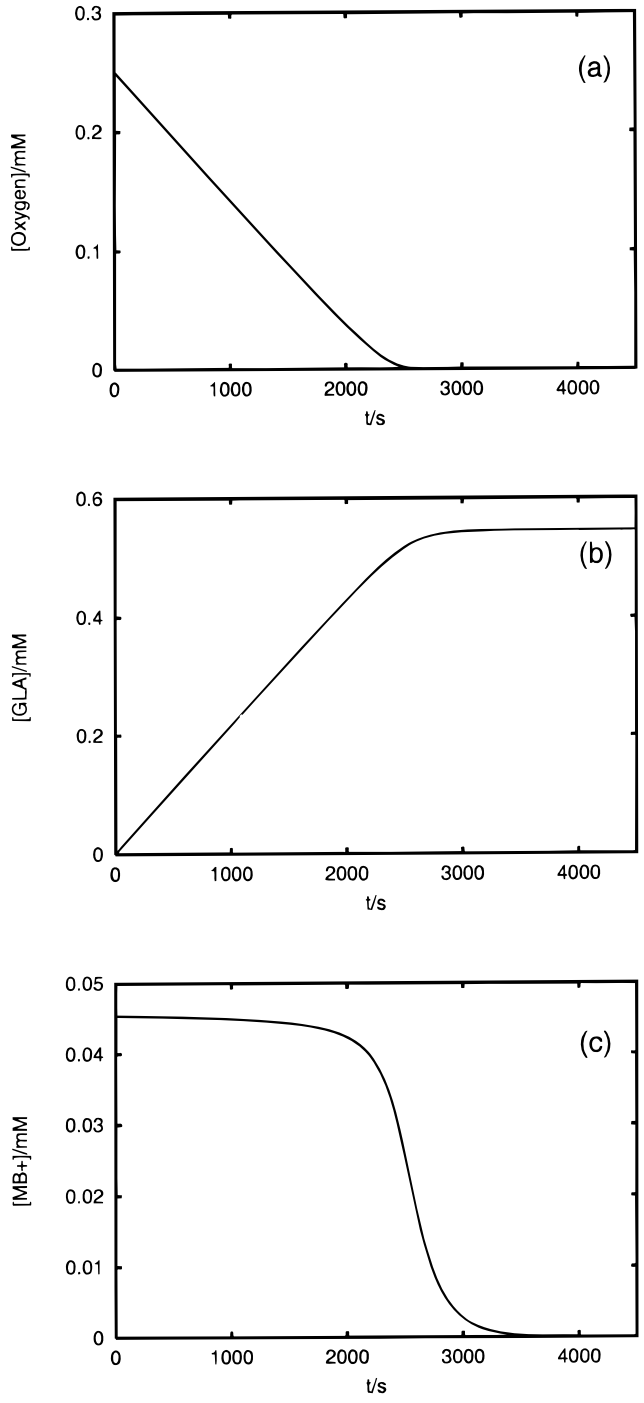

Figure 12. Theoretical calculations of the time dependence of the concentrations. Initial concentrations: $[OH^-] = 0.020$ M, $[MB^+] = 4.6 \times 10^{-5}$ M, [GL] = 0.054 M. (a) $[O_2]$ (see Figure 3).(b) [GLA]. (c) $[MB^+]$.

To test this hypothesis we performed an experiment which displays pattern formation in a solution without a free surface. This system had a membrane preventing evaporation while allowing the oxygen to diffuse into the system. The reaction chamber consisted of a Petri dish with a permeable bottom which was filled completely with reaction mixture, inverted, and placed in the thermostat filled with an atmosphere of pure O_2. This extra supply of O_2 was needed to increase the amount of O_2 diffusing through the membrane. After approximately 1 h an instability occurred and after some time the pattern shown in Figure 16a developed.

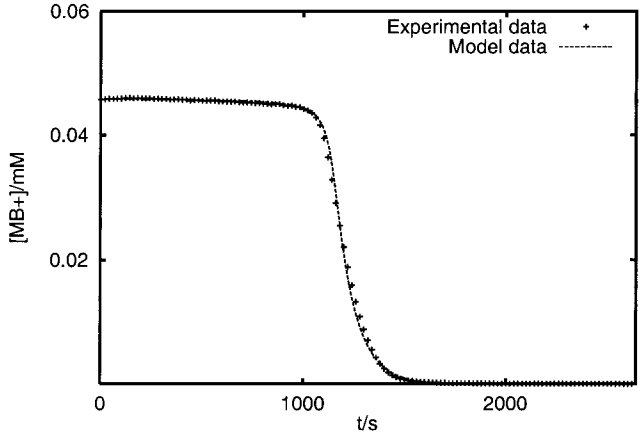

Figure 13. Comparison of a set of experimental data and data obtained from a fit of the kinetic model.

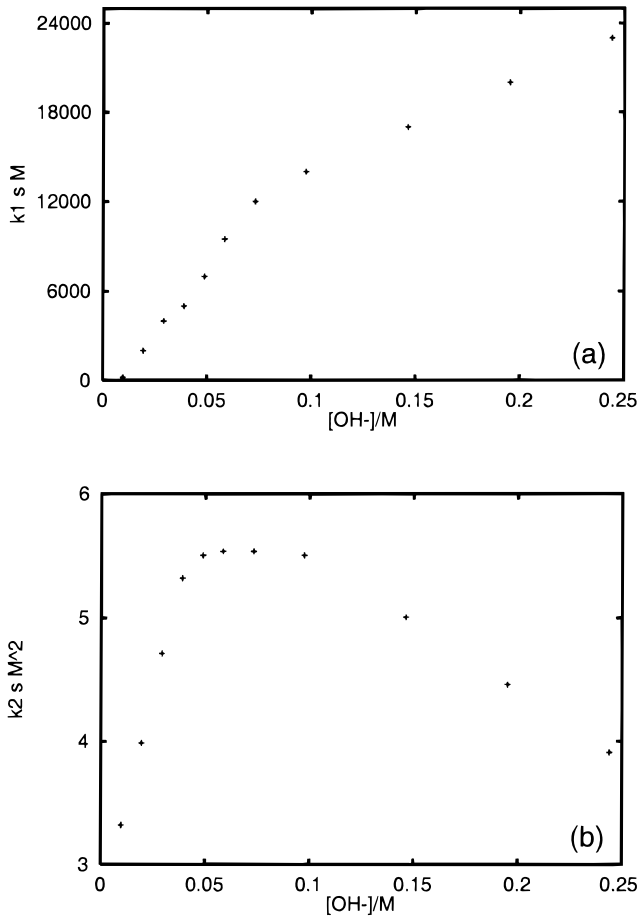

Figure 14. Rate constants k_1 and k_2 vs $[OH^-]$. These constants are obtained by fitting the model to the experimental data. (a) k_1. (b) k_2.

As another test to stress the role of an overturning instability we performed the experiment shown in panel (b) of Figure 16. A cuvette completely filled with reaction mixture was covered with a lid having a little hole through which oxygen could diffuse. The mixture started blue as usual and then, after a while, it became colorless and a blue plume sank from the hole to the bottom of the cuvette.

7. Conclusions

In this paper we have investigated the different kind of patterns that appear in "the blue bottle" system with a variety of experimental conditions. We have seen that two different

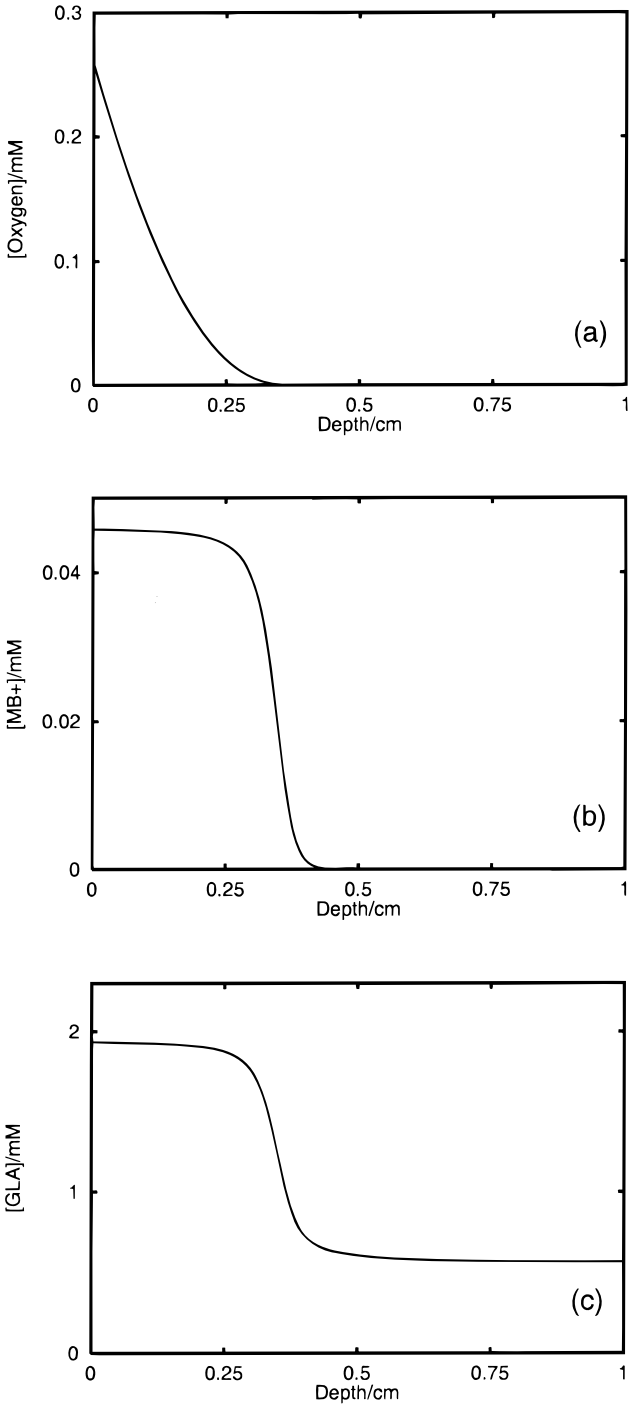

Figure 15. Steady-state profiles of the different concentration variables vs depth. The profiles were obtained by solving the full reaction diffusion equations neglecting the diffusion of MB^+ and gluconic acid and assuming a constant concentration of O_2 at the surface (as explained in section 5). (a) $[O_2]$ vs depth. (b) $[MB^+]$ vs depth. (c) [GLA] vs depth.

shapes—lines and dots—are typical. Often, they appear mixed in the same pattern, but in other cases one type is clearly dominant over the other.

After its emergence, the pattern remains stationary for a time of the order of 1 h before it gradually disappears. The shape and position of the convection cells usually changes very little, except that lines usually break into dots after some time.

We have proposed a reduced kinetic model that, in the range of concentrations we have used, reproduce the chemical behavior of the system well. Other more detailed models have been suggested by Adamčiková et al.[17] By fitting our simple model to the experimental data we have been able to determine the rate constants of the model.

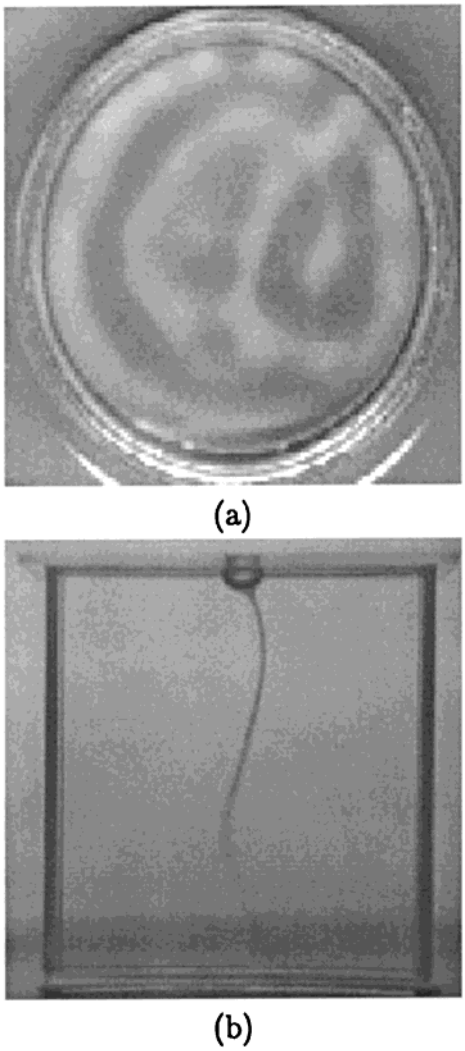

Figure 16. (a) Pattern developed in a Petri dish after approximately 5000 s where the free surface has been substituted with an oxygen-permeable membrane. The diameter of the Petri dish is 5.1 cm. (b) A plume of oxygen-rich fluid sinking to the bottom of a completely filled cuvette from a small hole in the lid. Width = 6.3 cm, height = 6.7 cm, and thickness = 1.3 cm.

We have measured the density of different solutions of glucose and gluconic acid. It was found that the solutions of gluconic acid are denser than equimolar solutions of glucose, strongly suggesting that gradients in density control the appearance of the instability.

We have calculated the concentration/depth profile using the simple model in a one-dimensional reaction−diffusion system maintaining a constant oxygen concentration at the upper boundary. The simulation helps explain the observation of a thin blue layer in the colorless system before the instability emerges.

Finally, we have performed two experiments that clearly support our overturning instability hypothesis.

A mathematical analysis of the key hydrodynamic instability mechanisms, for the theoretical prediction of pattern wavelengths, and direct numerical simulations shall be the subjects of forthcoming papers.

Acknowledgment. We thank Dr. Mads Ipsen for help with programming the reaction−diffusion simulation. This work was

supported by the TMR-Network on Patterns, Noise and Chaos, Project No. ERBFMRXCT960085.

References and Notes

(1) Matthiessen, K.; Wilke, H.; Müller, S. C. *Phys. Rev. E* **1996**, *53*, 6056.
(2) Pojman, J. A.; Epstein, I. R. *J. Phys. Chem.* **1990**, *94*, 4966.
(3) Masere, J.; Vasquez, D. A.; Edwards, B. F.; Wilder, J. W.; Showalter, K. *J. Phys. Chem.* **1994**, *98*, 6505.
(4) Borckmans, P.; Dewel, G.; Walgraef, D.; Katayama, Y. J. *Stat. Phys.* **1987**, *48*, 1031.
(5) Möckel, P. *Naturwissenschaften* **1977**, *64*, 224.
(6) Micheau, J. C.; Gimenez, M.; Borckmans, P.; Dewel, G. *Nature* **1983**, *305*, 43.
(7) Avnir, D.; Kagan, M. *Nature* **1984**, *307*, 717.
(8) Gambale, F.; Gliozzi, A. *J. of Phys. Chem.* **1972**, *76*, 783.
(9) Liu, C. Z.-W.; Knobler, C. M. *Physica A* **1992**, *181*, 243.
(10) Campbell, J. A. *J. Chem. Edu.* **1963**, *40*, 578.
(11) Adamčková, L.; Ševčík, P. *J. Chem. Educ.* **1998**, *75*, 1580.
(12) Adamčíková, L.; Ševčík, P. *Z. Naturforsch.* **1997**, *52a*, 650.
(13) Vandaveer, W. R.; Mosher, M. *J. Chem. Educ.* **1997**, *74*, 402.
(14) Childress, S.; Levandowsky, M.; Spiegel, E. A. *J. Fluid Mech.* **1975**, *63*, 591.
(15) Bees, M. A.; Hill, N. A. *J. Exp. Biol.* **1997**, *200*, 1515.
(16) Watzl, M.; Münster, A. F. *J. Phys. Chem. A* **1998**, *102*, 2540.
(17) Adamčíková, L.; Pavlíková, K.; Sevčík, P. *Int. J. Chem. Kinet.* **1999**, *31*, 463.